Advanced glycation end-products promote hepatosteatosis by interfering with SCAP-SREBP pathway in fructose drinking mice

Raffaella Mastrocola[1], PhD, Massimo Collino[2], PhD, Mara Rogazzo[2], PhD student, Claudio Medana[3], PhD, Debora Nigro[1], PhD student, Giuseppe Boccuzzi[4], MD, Manuela Aragno[1], PhD.

Affiliations: [1]Department of Clinical and Biological Sciences, Experimental Medicine and Clinical Pathology Unit, University of Turin, Italy; [2]Department of Drug Science and Technology, University of Turin, Turin, Italy; [3]Department of Molecular Biotechnology and Life Sciences, University of Turin, Italy; [4]Oncological Endocrinology, University of Turin, Italy.

Author contribution: experiments planning and manuscript drafting: RM, MA, and GB; animal treatment: RM and MC; analytical chemistry studies: CM; biochemical parameters detection and biomolecular techniques: DN and MR.

Corresponding author:
Raffaella Mastrocola, PhD
Dept. of Clinical and Biological Sciences
Experimental Medicine and Clinical Pathology Unit
University of Turin - C.so Raffaello 30 - 10125 Torino, Italy
Tel: +390116707758 - Fax: +390116707753
E-mail address: raffaella.mastrocola@unito.it

Running head title: AGEs induce SREBP1c activation

Abstract

Clinical studies have linked the increased consumption of fructose to the development of obesity, dyslipidemia and impaired glucose tolerance, and a role in hepatosteatosis development is presumed. Fructose can undergo a non-enzymatic reaction from which advanced glycation endproducts (AGEs) are derived, leading to the formation of dysfunctional, fructosylated proteins, however the *in vivo* formation of AGEs from fructose is still less known than that from glucose.

In the present study C57Bl/6J mice received 15% (w/v) fructose (FRT) or 15% (w/v) glucose (GLC) in water to drink for 30 weeks, resembling human habit to consume sugary drinks. At the end of protocol both FRT and GLC drinking mice had increased fasting glycaemia, glucose intolerance, altered plasma lipid profile, and marked hepatosteatosis. FRT mice had higher hepatic triglycerides deposition than GLC, paralleled by a greater increased expression and activity of the sterol regulatory element-binding protein 1 (SREBP1), the transcription factor responsible for the *de novo* lipogenesis, and of its activating protein SCAP. LC-MS analysis showed a different pattern of AGEs production in liver tissue between FRT and GLC mice, with larger amount of carboxymethyl lysine (CML) generated by FRT. Double immunofluorescence and coimmunoprecipitation analysis revealed an interaction between CML and SCAP that could lead to prolonged activation of SREBP1.

Overall, the high levels of CML and activation of SCAP/SREBP pathway associated to high fructose exposure here reported may suggest a key role of this signaling pathway in mediating fructose-induced lipogenesis.

Introduction

Many clinical studies have linked the rising consumption of soft drinks added with fructose to the development of obesity, dyslipidemia, insulin resistance, impaired glucose tolerance, and hypertension in adults (6,9,19, 26). Interestingly, clinical data show that inclusion of fructose in the diet for 10 weeks leads to a greater increase in hepatic lipid synthesis than that occurring with an equal amount of glucose (42).

Lipid metabolism is regulated by the sterol regulatory element binding proteins (SREBP) family, comprising three subtypes: SREBP-1a and SREBP-1c, which are generated by alternative splicing, and SREBP-2. SREBP-1c, expressed in most tissues with a greater prevalence than SREBP1a in liver and adrenal glands, is in charge of governing fatty acid and triacylglyceride metabolism, while SREBP-2, ubiquitously expressed, is involved in the regulation of cholesterol metabolism. Both SREBP-1 and SREBP-2 are synthesized as membrane proteins in the endoplasmic reticulum (ER) forming a complex with the SREBP-cleavage activating protein (SCAP). In spite of the distinct roles of the SREBPs in lipid metabolism, they are both subjected to the identical processing pathway (37): when TG or cholesterol synthesis are required, SCAP shuttles SREBPs from the endoplasmic reticulum (ER) to the Golgi, where they are cleaved by two proteases and enter the nucleus, bind to the sterol-regulatory elements in the promoters of target genes and increase transcription of lipogenic or cholesterologenic enzymes (17). Interestingly, SREBP-1 and SREBP-2 processing is triggered by different types of stimuli: while SREBP-1 activation depends primarily on insulin signaling and nutritional status, SREBP-2 is sensitive to membrane sterols level (37).

The liver is the main organ in which fructose metabolism takes place rapidly leading to increased hepatic synthesis of glycogen, fatty acids and triglycerides (TG) (45). Nonalcoholic fatty liver disease (NAFLD) is the most common disorder in industrialized countries, affecting 15-20% of the general population (49) and epidemiological studies have indicated that the development of NAFLD may be associated with excessive fructose consumption (35,50).

3

86   Among the chemical properties of fructose, a non-enzymatic pathway known as the Maillard

87   reaction is reported, in which fructose reacts with the aminic groups of proteins. After this reaction,

88   the anomerisation equilibrium of fructose is displaced toward the open form of the sugar, which is

89   highly reactive, especially compared to the forms derived from glucose (43). The Maillard reaction

90   is also one of the "classic" pathways from which the advanced glycation endproducts (AGEs) are

91   derived. It is known that a mixed class of toxic AGEs can be produced from the reduction of

92   glucose (49): CML (carboxymethyl lysine) and pentosidine are obtained through an oxidative

93   process, while MGO (methylglyoxal) and GLAP (glyceraldehyde-derived pyridinium compound)

94   through a non-oxidative process. Additionally, glucose is known to form AGE alpha-oxoaldehydes,

95   including GOLD (glyoxal-lysine dimer) and MOLD (methylglyoxal-lysine dimer), through the

96   polyol pathway (41). AGEs can exert a direct interference with cellular proteins function or a

97   receptor-mediated action, the latter being chiefly attributed to bonding with RAGE (Receptor for

98   AGE) (4). The interaction between AGEs and RAGE leads to intracellular signals responsible for

99   activation of pro-inflammatory transcription factors, such as NFkB (nuclear factor-kB) (3).

100   The Maillard reaction undertaken by fructose leads to the formation of altered, fructosylated

101   proteins, which are potentially toxic, indicating that fructose, together with glucose, plays an

102   important role in the formation of AGEs. So far, the *in vivo* formation of fructose-derived AGEs has

103   only been demonstrated in one study, and only through immunochemical analysis, without

104   reporting a description of their chemical structure (44). Thus, the chemical structure and toxicity of

105   AGEs molecules specifically derived from fructose are less well known than those derived from

106   glucose.

107   It might be hypothesized that the entrance of fructose in hepatocytes, where fructose is metabolized,

108   leads to the fructosylation of cytoplasmic proteins, causing a loss of their functionality and

109   regulation, thus contributing to liver alterations.

110   This study is aimed to characterized fructose-derived AGEs and to investigate their target proteins

111   in liver by a comparative analysis between fructose and glucose-drinking mice.

Materials and Methods

All compounds were purchased from Sigma Chemical Co. (St. Louis, MO, USA) and all primary antibodies were from Santa Cruz Biotechnology (Santa Cruz, CA, USA), unless otherwise stated.

Animals and treatments

Male C57Bl6/N mice (Charles River Laboratories, Calco, LC, Italy) aged 5 weeks were cared for in compliance with the European Council directives (No. 86/609/EEC) and with the Principles of Laboratory Animal Care (NIH No. 85–23, revised 1985). The scientific project was approved by the local ethical committee. The animals were divided into three groups of 8-10 mice: CTRL-group, drinking tap water; FRT-group, drinking a 15% fructose solution; GLC-group, drinking a 15% glucose solution. All groups were fed with a standard lab chow and received drink and food *ad libitum*.

Body weight, drink and food intake were recorded weekly. Fasting glycemia was measured at the start of the protocol and every 8 weeks by saphenous vein puncture using a glucometer (GlucoGmeter, Menarini Diagnostics, Firenze, Italy). After 30 weeks mice were anesthetized and killed by cardiac exsanguination. Blood was collected and plasma isolated. The liver was rapidly removed. A portion was cryoprotected in OCT (Optimal Cutting Temperature) compound (VWR, Milano, Italy) and frozen in N_2 for cryostatic preparations. Other portions were frozen in N_2 and stored at $-80°C$ for protein analysis.

Oral glucose tolerance test

Before killing, a glucose solution was administered orally at 2 g/kg b.w after a fasting period of 6 h. Plasma glucose levels were measured every 30 minutes for 2 hrs after glucose loading.

Biochemical parameters

Plasma lipid profile was determined by standard enzymatic procedures using reagent kits (triglycerides (TG), cholesterol, high-density lipoproteins (HDL), low-density lipoproteins (LDL): Hospitex Diagnostics, Florence, Italy; non-esterified fatty acid (NEFA): Wako Chemicals,Neuss, Germany).

138 Plasma insulin level was measured using an enzyme-linked immunosorbent assay (ELISA) kit

139 (Mercodia AB, Uppsala, Sweden).

140 For tissue TG and cholesterol content determination, colorimetric assay kits were used after lipid

141 extraction (TG: Triglyceride Quantification Kit, Abnova Corporation, Aachen, Germany;

142 cholesterol: Hospitex Diagnostics).

143 **Oil red staining**

144 Liver lipid accumulation was evaluated by oil red staining on 4 μm cryostatic sections. Stained

145 tissues were viewed under an Olympus Bx4I microscope (10x magnification) with an

146 AxioCamMR5 photographic attachment (Zeiss, Gottingen, Germany). The sections were analyzed

147 on six fileds/slide and scored by a blinded pathologist using the NAFLD activity score (NAS)

148 system (21).

149 **Preparation of tissue extracts**

150 Liver cytosolic, nuclear, and total proteins were extracted as previously described (28). Protein

151 content was determined using the Bradford assay and samples were stored at -80°C until use.

152 **AGEs analysis with LC-MS**

153 Pentosidine, GOLD, MOLD, CML, and GLAP, were evaluated on total liver extracts after

154 hydrolisis with 0.6 M trichloroacetic acid and 50 μL of hydrochloric acid 6 M for 12 hours at 60°C.

155 The chromatographic separations were run on an Ultimate 3000 HPLC (Dionex, Milan, Italy)

156 coupled to a high resolving power mass spectrometer (HRMS) LTQ Orbitrap (Thermo Scientific,

157 Rodano, Italy), equipped with an atmospheric pressure interface and an ESI ion source. The

158 samples were analyzed using an Reverse Phase C18 column (Phenomenex Synergi 150×2.1 mm, 3

159 μm particle size) at a flow rate of 200 μL/min. A gradient mobile phase composition was adopted:

160 95/5 to 40/60 in 25 min, 5 mM heptafluorobutanoic acid/acetonitrile. The monitored protonated

161 molecular ions were 205.1188 *m/z* for CML, 255.1344 *m/z* for GLAP, 341.2189 *m/z* for MOLD,

162 327.2032 *m/z* for GOLD and 379.2094 *m/z* for pentosidine. Quantitative determination of all the

163 analytes were done by using pentosidine calibration data.

Western blotting.

Equal amounts of total, cytosolic or nuclear proteins were separated by SDS-PAGE and electrotransferred to nitrocellulose membrane (GE-Healthcare Europe, Milano, Italy). Mouse anti-NFkBp65, rabbit anti-SREBP1 and mouse anti-SREBP2 antibodies were probed on both cytosolic and nuclear extracts. Goat anti-ICAM-1 (intercellular adhesion molecule-1) and anti-CTGF (connective tissue growth factor), rabbit anti-SCAP, anti-ACC (Cell Signaling Technology, Danver, MA,USA), anti-HMGR (Millipore, Temecula, CA, USA), anti-apoB, anti-CPT1-L, and anti-RAGE were probed on total extracts. Rabbit anti-apoB was also probed on 10 ul of plasma samples. Proteins were detected with ECL chemiluminescence substrate (GE-Healthcare) and quantified by densitometry using analytic software (Quantity-One, Bio-Rad). β-actin served as loading control for total and cytosolic protein extracts, and lamin-B1 for nuclear extracts.

Immunofluorescence

Localization of SCAP, SREBP1, CML and MGO was assessed on 4 μm liver cryostatic sections by indirect immunofluorescence. Sections were blocked for 1 h with 3% BSA in PBS added with unconjugated goat anti-mouse IgG to prevent mouse-on-mouse interferences. Thus, sections were incubated overnight with rabbit anti-SCAP, rabbit anti-SREBP1, mouse anti-CML (Trans-Genic, Kobe, Japan) or mouse anti-MGO (Trans-Genic) primary antibodies and for 1 h with fluorescent secondary antibodies (Dako, Glostrup, Denmark): TRITC-conjugated anti-rabbit IgG or biotin-conjugated anti-mouse IgG followed by FITC-conjugated streptavidin. Negative controls were prepared incubating sections with secondary antibodies. Sections were examined using a Leica Olympus epifluorescence microscope (Olympus Bx4I) and digitised with a high resolution camera (Zeiss).

Double immunofluorescence.

Double immunofluorescence was performed for SCAP and CML on liver cryostatic sections. After blocking, sections were incubated with a mix of primary antibodies for 1 hour. After washing, sections were incubated with a mix of labelled secondary antibodies. The images were colour-

7

190 combined and assembled into photomontages by using Adobe Photoshop (Universal Imaging, West

191 Chester, PA).

Co-immunoprecipitation.

193 Equal amounts of total proteins (500 μg) were incubated overnight with SCAP rabbit-polyclonal

194 antibody (2 μg). The antibody-antigen complexes were then incubated with fresh Protein A

195 Sepharose beads for 3 h. SDS Laemmli buffer was added to the beads and eluted proteins were

196 subjected to SDS–PAGE and immunoblotted with mouse anti-CML monoclonal antibody and, after

197 stripping, with rabbit anti-SCAP antibody.

Statistical analysis

199 All values are expressed as means ± SD and were analyzed by Anova test followed by Bonferroni's

200 post-test. A *P* value <0.05 was considered statistically significant.

Results

Fructose and glucose drinking in mice induces alterations in body weight, glucose tolerance
and plasma lipid profile.

204 The daily drink intake in the FRT and GLC drinking groups was markedly higher than in the CTRL

205 group, drinking tap water. Moreover, GLC intake was also significantly higher than FRT, but

206 despite that, the total daily caloric intake was similar among the groups, being proportionally

207 reduced the food intake (**Table 1**).

208 As shown in **Table 1**, mice drinking FRT or GLC for 30 weeks showed a significant increase in

209 body weight compared to CTRL mice (+31%).

210 Fasting glycemia was significantly higher both in FRT and in GLC groups compared to CTRL

211 group (**Table 1**). During OGTT **(Fig. 1A)**, the glycemic curves of FRT and GLC mice were

212 markedly moved away from CTRL curve at every time-point after glucose charge. Plasma insulin

213 level was slightly increased in GLC group and in a greater extent in FRT group, with respect to

214 CTRL, without reaching any statistical significance (**Table 1**).

8

215 In comparison with CTRL animals, FRT mice showed alterations in plasma lipid profile (**Table 2**)

216 featured by increased levels of TG (+43%), cholesterol (+37%), and LDL (+80%), paralleled by a

217 decrease in NEFA (-24%). GLC mice only showed a trend to dyslipidemia that didn't reach the

218 statistical significance, excepting for HDL level (-16%), and for NEFA level that, conversely to

219 FRT group, was increased (+20%) compared to CTRL.

220 **Fructose and glucose drinking increases liver TG and cholesterol content and induces**

221 **hepatosteatosis.**

222 Hepatic homogenates of FRT mice showed a marked increase in TG and cholesterol content

223 compared to CTRL (+100% and +50%, respectively). In liver homogenates from GLC mice an

224 increase in cholesterol content similar to FRT was found (+42% of the CTRL value), while the TG

225 level tend to increase compared to CTRL, but remained significantly lower than in FRT group (-

226 60%) (**Fig. 1B**).

227 Oil red staining of liver sections (**Fig. 1C-E**) highlighted a marked lipid deposition both in FRT (**D**)

228 and in GLC mice (**E**) compared to CTRL (**C**), resembling a condition of non-alcoholic fatty liver

229 disease, with different histopathological features. FRT mice liver showed enlarged hepatocytes with

230 periportal macrovacuolar steatosis. In contrast, liver of GLC mice showed a microvesicular steatosis

231 with a panlobular dissemination. A significantly higher steatosis grade was detected in FRT

232 compared to GLC mice, conferring an overall NAS score of 5.2±1.3 to FRT vs. 3.8±0.9 to GLC

233 mice liver (P<0.05) (**Fig. 1F**).

234 **Fructose and glucose drinking enhances TG and cholesterol synthesis through activation of**

235 **SCAP-SREBP signalling.**

236 To further investigate the greater lipogenic effect of FRT with respect to GLC, we assessed the

237 expression and activation of SREBP1c, SREBP2 and their activating protein SCAP by western

238 blotting analysis (**Fig. 2**).

239 SCAP was markedly up-regulated in FRT and GLC mice compared to CTRL (**Fig. 2A,B**), in a

240 significantly greater extent in FRT than in GLC. Both SREBP1c and SREBP2 were up-regulated in

9

FRT and GLC groups compared to CTRL (**Fig. 2C-H**). Specifically, the 68 kDa active form (**Fig. 2C,E**) and the 125 kDa inactive form (**Fig. 2F,H**) of SREBP1c were significantly more expressed in liver of FRT mice than in GLC. In contrast, SREBP2 was equally activated in FRT and GLC liver (**Fig. 2D,E**), while inactive form of SREBP2 was more expressed in GLC liver than in FRT, without reaching significant difference (**Fig. 2G,H**). The activation of the SCAP/SREBP pathway is confirmed by the increased expression in FRT and GLC mice liver of both the SREBP1c target gene encoding acetyl coenzyme A carboxylase (ACC), one of the enzymes that promote triglyceride synthesis, (**Fig. 3A,B**), and the SREBP2 target gene encoding hydroxymethyl coenzyme A reductase (HMGR), the rate limiting enzyme of the cholesterol synthesis (**Fig. 3C,D**). Notably, the expression of ACC is about 35% greater in FRT than in GLC mice liver (**Fig. 3B**) according to the higher activation of SREBP1c.

ApoB100 protein level was measured in plasma and liver as marker of VLDL secretion (**Fig. 3E**), while the expression of carnitine palmitoyl transferase 1 (CPT1-L) (**Fig. 3G**) indicates the efficiency of β-oxidation. Any significant differences were seen in ApoB100 plasma-to-liver protein level (**Fig. 3F**) and in liver expression of CPT1-L (**Fig. 3H**), among the three groups, although a trend to a reduction of CPT1-L level was seen in GLC mice.

Fructose and glucose drinking enhances AGEs generation and activates RAGE signalling.

As shown in **Table 3**, all AGEs here measured were markedly increased in liver homogenates of FRT and GLC mice compared to CTRL. Most notably, GLAP and MOLD highest levels were detected in the liver of GLC-drinking group, while GOLD and CML were produced in the greatest amount in the liver from FRT group (**Table 3**). The receptor for AGEs, RAGE, was up-regulated both in FRT and GLC mice compared to CTRL (+100%) (**Fig. 4A,B**) and the downstream signalling was activated as demonstrated by the nuclear translocation of NFkB-p65 (**Fig. 4C,D**). As consequence, we found increased levels of the NF-kB-dependent protein ICAM-1 in both sugar-drinking groups (**Fig. 4E,F**), and a slight, but not significant, increase of an early marker of fibrosis,

266 CTGF (**Fig. 4E,F**), even if morphological signs, as collagen I and IV deposition, were still not

267 detectables (data not shown).

268 **CML colocalizes with SCAP in liver of fructose drinking mice.**

269 Immunofluorescence analysis on liver sections from FRT mice showed a prevalent nuclear

270 localization for SREBP1c **(Fig. 5A,B)**, consistent with its activation, and a cytosolic perinuclear

271 localization for SCAP (**Fig. 5D,E**). CML localized mainly in cytosol of hepatocytes (**Fig. 5G,H**),

272 with a perinuclear distribution similar to SCAP. Interestingly, MGO was detected mainly in the

273 endothelium and at the plasmamembrane of hepatocytes (**Fig. 5J,K**).

274 Double immunofluorescence studies in liver of FRT group confirmed that CML colocalizes with

275 SCAP in the perinuclear zone of the hepatocytes (**Fig. 6A-F**).

276 **CML modifies SCAP in liver of fructose drinking mice.**

277 Finally, co-immunoprecipition assay has been performed to evaluate SCAP glycosylation by

278 CML (**Fig. 6G,H**). SCAP was immunoprecipitated with Protein A Sepharose, electrophoresed and

279 blotted on nitrocellulose membrane. Membrane was then exposed to CML antibody, revealing a

280 complex between SCAP and CML in liver of FRT mice.

281 **Discussion**

282 This study clearly demonstrates a significant activation of SCAP/SREBP pathway and the

283 following increase in *de novo* lipogenesis, which were associated to high levels of fructose-derived

284 AGEs in the liver of mice chronically exposed to high fructose intake.

285 Reducing sugars, as fructose and glucose, react spontaneously with amino groups of proteins to

286 advanced glycation end products (AGEs) (27). Although glucose plays a primary role in the

287 formation of AGEs, it is now known that fructose undergoes the same non-enzymatic glycation

288 reaction at a much faster rate. When fructose assumption with foods or beverages is remarkable, its

289 high reactivity may substantially contribute to the tissue formation of AGEs and lead to cellular

290 alterations and dysfunction (38).

291 Our study shows for the first time a different pattern of hepatic AGEs between FRT and GLC

292 detected by LC-MS. In detail, FRT generates higher levels of AGEs derived from glyoxal, such as

293 GOLD and CML, while we found more AGEs derived from methylglyoxal, MOLD and GLAP, in

294 GLC mice. These differences may just reflect the dissimilar pathways and rates of FRT and GLC

295 metabolism. Moreover, methylglyoxal is less toxic toward hepatocytes than glyoxal being a better

296 substrate for the carbonyl detoxifying enzymes, while the rate of metabolism of glyoxal by

297 hepatocyte metabolizing enzymes is much faster than for methylglyoxal (39). This could account

298 for the greater accumulation of GOLD and CML in FRT mice.

299 So far there are limited data directly comparing the effects of fructose and glucose *in vivo* on lipid

300 metabolism, the few existing using very high concentration of sugars for a short time (22,40,42,48),

301 and even less on AGEs generation (1,27).

302 For this reason, the peculiarities of the present study are the characterization of *in vivo* AGEs

303 generation from fructose and the suggestion of their involvement in the increased hepatic lipid

304 synthesis, in comparison with glucose, through an experimental protocol based on low sugar

305 concentrations given for a long time, mimicking the diffused human habit to daily drink sweetened

306 beverages.

307 In physiological conditions, the potential sources of TG that contribute to fatty liver development

308 are NEFA coming from the hydrolysis of fatty acids stored in adipose tissue, dietary fatty acids and

309 newly synthesized fatty acids through *de novo* lipogenesis (11). Moreover, an impairment of the

310 lipid β-oxidation rate or of the hepatic triglycerides clearance by VLDL may also lead to hepatic

311 lipid accumulation (46). In the present study FRT drinking mice had lower plasma NEFA than GLC

312 mice, while both the liver expression of CPT-1, the rate limiting enzyme of mitochondrial β-

313 oxidation, and the ratio between plasma and liver levels of ApoB100, the structural component of

314 VLDL, did not differ in FRT and GLC mice. These data indicate for the first time that the *de novo*

315 synthesis is the main pathway responsible for the higher lipid accumulation in liver of FRT mice

316 with respect to GLC, in which other mechanisms, such as reduction of β-oxidation and higher

317 hydrolysis of adipose fat, may contribute to hepatic steatosis, as previously suggested by other

318 authors (30).

319 Liver is the main tissue involved in fructose handling and *de novo* lipogenesis (18), and many

320 studies have shown that fructose plays a specific role in the pathogenesis of hepatosteatosis and

321 metabolic syndrome due to differential hepatic fructose metabolism (25,32,33). However, the

322 molecular mechanisms by which high fructose diets induce abnormalities in liver TG metabolism

323 are not fully understood.

324 It has been observed that a simultaneous induction of glycolitic and lipogenic genes is a salient

325 feature when dietary glucose is replaced with fructose. Indeed, fructose ingestion at high doses

326 increases expression of the genes encoding for lipogenic enzymes via the activation of SREBP1 in

327 the liver (29). Thus, we have analyzed the expression of SREBP1c, SREBP2 and of their chaperone

328 protein SCAP in the liver of FRT and GLC drinking mice.

329 In our work, chronic exposure to low levels of both FRT and GLC induced the activation of the

330 SCAP/SREBP system. Notably, there was a marked difference in SCAP expression between FRT

331 and GLC mice, being higher in FRT, and this could be crucial for the greater induction of

332 lipogenesis by fructose. Indeed, we observed a significantly higher expression and activation of

333 SREBP1c in liver of FRT versus GLC mice, as confirmed by the resulting higher expression of

334 ACC and by the greater hepatic TG accumulation. On the other hand, SREBP2 is equally

335 hyperactivated in FRT and GLC mice, leading thus to similar expression of HMGR and thereby to

336 similar level of cholesterol in liver. Although SCAP is the common activating protein of both

337 SREBP1c and SREBP2, the existence of unidentified regulatory factors, such as nutritional status or

338 food composition, that determine the fate of the SREBP/SCAP complex by distinguishing between

339 SREBP-1c and SREBP-2 processing, has been supposed (17,37).

340 Insulin is a well-known inducer of SREBP1c activity and hyperinsulinemia may contribute in

341 hyperactivation of lipogenic pathway (7,8). However, in our experimental model FRT and GLC

342 mice, even showing altered glucose homeostasis, didn't reach a condition of hyperisulinemia

343 adequate to induce the *de novo* lipogenesis.

344 We then hypothesized a possible interference of CML on SCAP/SREBP system. Indeed, a direct

345 correlation between AGEs serum level and triglyceride level was found in children and adolescent

346 with Type I diabetes (13). Besides, the generation of CML has been observed during high fat/high

347 sugar diets (20,36) and this has been attributed to lipid peroxidation processes (12). A relationship

348 between intracellular lipid accumulation and increase in CML levels has also been recently

349 demonstrated in an *in vitro* model of steatosis (12). Moreover, CML accumulation in the liver of

350 obese individuals has been involved in hepatosteatosis development (41). This is also supported by

351 a study showing that administration of pyridoxamine, an inhibitor of CML formation, reduces

352 plasma triglyceride and cholesterol on Zucker obese rats (2).

353 Several studies have indicated that interaction of CML with RAGE causes oxidative stress and

354 activation of NFkB via multiple intracellular signal pathways (5,16). Our results demonstrated that

355 both FRT- and GLC-chronic exposure increased hepatic RAGE expression, and consequently

356 activates NFkB and inflammatory/fibrogenic signaling, at the same level. Therefore, the CML

357 involvement in the higher lipogenesis occurring in FRT mice is not mediated by RAGE binding.

358 A recent *in vitro* study in cultured mesangial cells highlights a direct causal role for CML in

359 SREBPs activation by interfering with SCAP and thus driving SREBPs factors to elude its negative

360 feedback control (52). The glycosylation of SCAP by Golgi enzymes plays an important role in the

361 cycling of SCAP between the ER and the Golgi (31,51). In physiological conditions, high

362 intracellular concentrations of cholesterol prevent transport of the SCAP-SREBP complex from the

363 ER to the Golgi and downregulate SREBPs activation avoiding intracellular cholesterol and lipids

364 overloading (10). CML administration in mesangial cells disrupted the SCAP-mediated feedback

365 regulation of SREBPs, increasing SCAP gene transcription and protein stability, thereby enhancing

366 the cycling of SCAP between the ER and the Golgi and prolonging SREBPs activation (52).

367 Consistently, our immunofluorescence analysis suggested an interaction between CML and SCAP

which were extensively colocalized in the perinuclear zone of the hepatocytes in FRT mice. The result of coimmunoprecipitation technique further reinforced our hypothesis of a cross-link between CML and SCAP, indicating for the first time that a specific interference of CML in SCAP/SREBP system occurs also *in vivo* and, most notably, could be induced by FRT drinking. However, further experiments with specific CML inhibitors are needed for a conclusive demonstration of the causal role of fructose-derived AGEs in the activation of this specific signaling pathway. Recently, uric acid that generates from fructose metabolism has been suggested as a further mechanism contributing at least in part to the lipogenic effect of fructose feeding (23,24). Uric acid has been shown to induce mitochondrial oxidative stress and accumulation of citrate being the substrate for the *de novo* lipogenesis (23). It is known that oxidative stress is an important element in the glycoxidation process that leads to AGEs accumulation (15) and in some cases a direct positive correlation between uric acid and pentosidine levels has been reported (14,34).

In summary, the present results improve our knowledge on fatty liver development and show an association between high levels of fructose-derived AGEs and activation of *de novo* lipogenesis, thus suggesting more caution in the even wider employment of fructose as added sweetener in foods and beverages.

Grants

Disclosures

No conflict of interest, financial or otherwise, are declared by the authors.

References

1) Ahmed N, Furth AJ. Failure of common glycation assays to detect glycation by fructose. *Clin Chem* 38(7): 1301-3, 1992.

2) Alderson NL, Chachich ME, Youssef NN, Beattie RJ, Nachtigal M, Thorpe SR, Baynes JW. The AGE inhibitor pyridoxamine inhibits lipemia and development of renal and vascular disease in Zucker obese rats. *Kidney Int* 63(6): 2123-33, 2003.

3) Aragno M, Mastrocola R, Medana C, Restivo F, Catalano MG, Pons N, Danni O, Boccuzzi G. Up-regulation of advanced glycated products receptors in the brain of diabetic rats is prevented by antioxidant treatment. *Endocrinology* 146: 5561-5567, 2005.

4) Bierhaus A, Humpert PM, Morcos M, Wendt T, Chavakis T, Arnold B, Stern DM, Nawroth PP. Understanding RAGE, the receptor for advanced glycation end products. *J Mol Med* 83: 876-86, 2005.

5) Bohlender JM, Franke S, Stein G, Wolf G. Advanced glycation end products and the kidney. *Am J Physiol Renal Physiol* 289: F645-59, 2005.

6) Bray GA. Soft drink consumption and obesity: it is all about fructose. *Curr Opin Lipidol* 21: 51-57, 2010.

7) Brown MS, Goldstein JL. Selective versus total insulin resistance. Cell Metab 7:95–96, 2008.

8) Choi SH, Ginsberg HN. Increased very low density lipoprotein (VLDL) secretion, hepatic steatosis, and insulin resistance. *Trends Endocrinol Metab* 22: 353–363, 2011.

9) Elliott SS, Keim NL, Stern JS, Teff K, Havel PJ. Fructose, weight gain, and the insulin resistance syndrome. *Am J Clin Nutr* 76: 911-22, 2002.

10) Espenshade PJ, Hughes AL. Regulation of sterol synthesis in eukaryotes. *Annu Rev Genet* 41: 401-27, 2007.

11) Ferré P, Foufelle F. Hepatic steatosis: a role for de novo lipogenesis and the transcription factor SREBP-1c. *Diabetes Obes Metab* 2: 83-92, 2010.

16

419 12) Gaens KH, Niessen PM, Rensen SS, Buurman WA, Greve JW, Driessen A, Wolfs MG, Hofker

420 MH, Bloemen JG, Dejong CH, Stehouwer CD, Schalkwijk CG. Endogenous formation of Nε-

421 (carboxymethyl)lysine is increased in fatty livers and induces inflammatory markers in an in

422 vitro model of hepatic steatosis. *J Hepatol* 56: 647-55, 2012.

423 13) Galler A, Müller G, Schinzel R, Kratzsch J, Kiess W, Münch G. Impact of metabolic control

424 and serum lipids on the concentration of advanced glycation end products in the serum of

425 children and adolescents with type 1 diabetes, as determined by fluorescence spectroscopy and

426 nepsilon-(carboxymethyl)lysine ELISA. *Diabetes Care* 26(9):2609-15, 2003.

427 14) Germanová A, Koucký M, Hájek Z, Parízek A, Zima T, Kalousová M. Soluble receptor for

428 advanced glycation end products in physiological and pathological pregnancy. *Clin Biochem*

429 43(4-5): 442-6, 2010.

430 15) Giacco F, Brownlee M. Oxidative stress and diabetic complications. *Circ Res* 107(9): 1058-70,

431 2010.

432 16) Goldin A, Beckman JA, Schmidt AM, Creager MA. Advanced glycation end products:

433 sparking the development of diabetic vascular injury. *Circulation* 114: 597-605, 2006.

434 17) Goldstein JL, Bose-Boyd RA, Brown MS. Protein sensors for membrane sterols. *Cell* 124: 35–

435 46, 2006.

436 18) Hellerstein MK, Schwarz JM, Neese RA. Regulation of hepatic de novo lipogenesis in humans.

437 *Annu Rev Nutr* 16: 523–557, 1996.

438 19) Hofmann SM and Tschop MH. Dietary sugars: a fat difference. *J Clin Invest* 119: 1089-1092,

439 2009.

440 20) Kanner J. Dietary advanced lipid oxidation endproducts are risk factors to human health. *Mol*

441 *Nutr Food Res* 51: 1094-101, 2007.

442 21) Kleiner DE, Brunt EM, Van Natta M, Behling C, Contos MJ, Cummings OW, Ferrell LD, Liu

443 YC, Torbenson MS, Unalp-Arida A, Yeh M, McCullough AJ, Sanyal AJ; Nonalcoholic

17

444   Steatohepatitis Clinical Research Network. Design and validation of a histological scoring

445   system for nonalcoholic fatty liver disease. *Hepatology* 41: 1313–1321, 2005.

446   22) Koo HY, Miyashita M, Cho BH, Nakamura MT. Replacing dietary glucose with fructose

447   increases ChREBP activity and SREBP-1 protein in rat liver nucleus. *Biochem Biophys Res*

448   *Commun* 390(2): 285-9, 2009.

449   23) Lanaspa MA, Sanchez-Lozada LG, Choi YJ, Cicerchi C, Kanbay M, Roncal-Jimenez CA,

450   Ishimoto T, Li N, Marek G, Duranay M, Schreiner G, Rodriguez-Iturbe B, Nakagawa T, Kang

451   DH, Sautin YY, Johnson RJ. Uric acid induces hepatic steatosis by generation of mitochondrial

452   oxidative stress: potential role in fructose-dependent and -independent fatty liver. *J Biol Chem*

453   287(48): 40732-44, 2012.

454   24) Lanaspa MA, Sanchez-Lozada LG, Cicerchi C, Li N, Roncal-Jimenez CA, Ishimoto T, Le M,

455   Garcia GE, Thomas JB, Rivard CJ, Andres-Hernando A, Hunter B, Schreiner G, Rodriguez-

456   Iturbe B, Sautin YY, Johnson RJ. Uric acid stimulates fructokinase and accelerates fructose

457   metabolism in the development of fatty liver. *PLoS One* 7(10): e47948, 2012.

458   25) Lim JS, Mietus-Snyder M, Valente A, Schwarz JM, Lustig RH. The role of fructose in the

459   pathogenesis of NAFLD and the metabolic syndrome. *Nat Rev Gastroenterol Hepatol* 7(5):

460   251-64, 2010.

461   26) Madero M, Perez-Pozo SE, Jalal D, Johnson RJ, Sanchez-Lozada LG. Dietary fructose and

462   hypertension. *Curr Hypertens Rep* 13: 29–35, 2011.

463   27) Makita Z, Vlassara H, Cerami A, BucalaR. Immunochemical detection of advanced

464   glycosylation end products in vivo. *J Biol Chem* 267: 5133-8, 1992.

465   28) Mastrocola R, Guglielmotto M, Medana C, Catalano MG, Cutrupi S, Borghi R, Tamagno E,

466   Boccuzzi G, Aragno M. Dysregulation of SREBP2 induces BACE1 expression. *Neurobiol Dis*

467   44: 116-24, 2011.

468   29) Mori T, Kondo H, Hase T, Murase T. Dietary phospholipids ameliorate fructose-induced

469   hepatic lipid and metabolic abnormalities in rats. *J Nutr* 141: 2003-9, 2011.

470   30) Ngo Sock ET, Lê KA, Ith M, Kreis R, Boesch C, Tappy L. Effects of a short-term overfeeding

471   with fructose or glucose in healthy young males. *Br J Nutr* 103(7): 939-43, 2010.

472   31) Nohturfft A, Bose-Boyd RA, Scheek S, Goldstein JL, Brown MS. Sterols regulate cycling of

473   SREBP cleavage-activating protein (SCAP) between endoplasmic reticulum and Golgi. *PNAS*

474   96: 11235–11240, 1999.

475   32) Nomura K, Yamanouchi T. The role of fructose-enriched diets in mechanisms of nonalcoholic

476   fatty liver disease. *J Nutr Biochem* 23:203-8, 2012.

477   33) Nseir W, Nassar F, Assy N. Soft drinks consumption and nonalcoholic fatty liver disease.

478   World *J Gastroenterol* 16: 2579-88, 2010.

479   34) Odetti P, Cosso L, Pronzato MA, Dapino D, Gurreri G. Plasma advanced glycosylation end-

480   products in maintenance haemodialysis patients. *Nephrol Dial Transplant* 10(11): 2110-3,

481   1995.

482   35) Ouyang X, Cirillo P, Sautin Y, McCall S, Bruchette JL, Diehl AM, Johnson RJ, Abdelmalek

483   MF. Fructose consumption as a risk factor for non-alcoholic fatty liver disease. *J Hepatol* 48:

484   993-9, 2008.

485   36) Ruiz-Ramírez A, Chávez-Salgado M, Peñeda-Flores JA, Zapata E, Masso F, El-Hafidi M.

486   High-sucrose diet increases ROS generation, FFA accumulation, UCP2 level, and proton leak

487   in liver mitochondria. *Am J Physiol Endocrinol Metab* 301: E1198-207, 2011.

488   37) Sato R, Sterol metabolism and SREBP activation. *Archives of Biochemistry and Biophysics*

489   501: 177–181, 2010

490   38) Schalkwijk CG, Stehouwer CD, van Hinsbergh VW. Fructose-mediated non-enzymatic

491   glycation: sweet coupling or bad modification. *Diabetes Metab Res Rev* 20: 369-82, 2004.

492   39) Shangari N, Poon R, O'Brien PJ. Hepatocyte methylglyoxal (MG) resistance is overcome by

493   inhibiting aldo-keto redictases and glyoxalase I catalysed MG metabolism. *Enzymol Mol Biol*

494   *Carbonyl Metab* 12: 266-275, 2006.

495   40) Silbernagel G, Machann J, Unmuth S, Schick F, Stefan N, Häring HU, Fritsche A. Effects of 4-

496   week very-high-fructose/glucose diets on insulin sensitivity, visceral fat and intrahepatic lipids:

497   an exploratory trial. *Br J Nutr* 106(1): 79-86, 2011.

498   41) Singh R, Barden A, Mori T, Beilin L. Advanced glycation end-products: a review.

499   *Diabetologia* 44: 129-46, 2001.

500   42) Stanhope KL, Schwarz JM, Keim NL, Griffen SC, Bremer AA, Graham JL, Hatcher B, Cox

501   CL, Dyachenko A, Zhang W, McGahan JP, Seibert A, Krauss RM, Chiu S, Schaefer EJ, Ai M,

502   Otokozawa S, Nakajima K, Nakano T, Beysen C, Hellerstein MK, Berglund L, Havel PJ.

503   Consuming fructose-sweetened, not glucose-sweetened, beverages increases visceral adiposity

504   and lipids and decreases insulin sensitivity in overweight/obese humans. *J Clin Invest* 119:

505   1322-1334, 2009.

506   43) Suarez G, Rajaram R, Oronsky AL, Gawinowicz MA. Nonenzymatic glycation of bovine

507   serum albumin by fructose (fructation). Comparison with the Maillard reaction initiated by

508   glucose. *J Biol Chem* 264: 3674-3679, 1989.

509   44) Takeuchi M, Iwaki M, Takino J, Shirai H, Kawakami M, Bucala R, Yamagishi S.

510   Immunological detection of fructose-derived advanced glycation end-products. *Lab Invest* 90:

511   1117-27, 2010.

512   45) Tappy L and Lê KA. Metabolic effects of fructose and the worldwide increase in obesity.

513   *Physiol Rev* 90: 23-46, 2010.

514   46) Tappy L, Lê KA. Does fructose consumption contribute to non-alcoholic fatty liver disease?

515   *Clin Res Hepatol Gastroenterol* 36(6): 554-60, 2012.

516   47) Targher G. Non-alcoholic fatty liver disease, the metabolic syndrome and the risk of

517   cardiovascular disease: the plot thickens. *Diabetologia* 51: 444-50, 2008.

518   48) Teff KL, Grudziak J, Townsend RR, Dunn TN, Grant RW, Adams SH, Keim NL, Cummings

519   BP, Stanhope KL, Havel PJ. Endocrine and metabolic effects of consuming fructose- and

520   glucose-sweetened beverages with meals in obese men and women: influence of insulin

521   resistance on plasma triglyceride responses. *J Clin Endocrinol Metab* 94(5): 1562-9, 2009.

522   49) Thornalley PJ, Battah S, Ahmed N, Karachalias N, Agalou S, Babaei-Jadidi R, Dawnay A.

523   Quantitative screening of advanced glycation endproducts in cellular and extracellular proteins

524   by tandem mass spectrometry. *Biochem J* 375: 581-92, 2003.

525   50) Thuy S, Ladurner R, Volynets V, Wagner S, Strahl S, Königsrainer A, Maier KP, Bischoff SC,

526   Bergheim I. Nonalcoholic fatty liver disease in humans is associated with increased plasma

527   endotoxin and plasminogen activator inhibitor 1 concentrations and with fructose intake. *J Nutr*

528   138: 1452-5, 2008.

529   51) Velasco A, Hendricks L, Moremen KW, Tulsiani DR, Touster O, Farquhar MG. Cell type-

530   dependent variations in the subcellular distribution of alpha-mannosidase I and II. *J Cell Biol*

531   122: 39–51, 1993.

532   52) Yuan Y, Zhao L, Chen Y, Moorhead JF, Varghese Z, Powis SH, Minogue S, Sun Z, Ruan XZ.

533   Advanced glycation end products (AGEs) increase human mesangial foam cell formation by

534   increasing Golgi SCAP glycosylation in vitro. *Am J Physiol Renal Physiol* 301: F236-43, 2011.

535

536

537

538

539

540

541

542

543

544

21

Figure captions

546 **Fig. 1. FRT and GLC drinking affect glycaemic control and liver lipid accumulation.** (A) Oral

547 glucose tolerance test performed on 6 hrs fasting mice after 30 weeks of water, FRT or GLC

548 drinking. (B) TG and cholesterol content in mice liver. (C-E) Representative 20x magnification

549 photomicrographs of oil red staining on liver sections from CTRL (C), FRT (D), and GLC (E) mice.

550 (F) Pathological grading in liver sections from CTRL, FRT and GLC mice according to the NAFLD

551 activity score system by Kleiner et al**.** (21). Data are means ± S.D. of 8-10 mice per group. *$P<0.05$,

552 **$P<0.01$ vs CTRL; †$P<0.05$ vs FRT.

553

554 **Fig. 2. Expression analysis on SCAP/SREBP pathway.** Western blotting analysis for SCAP (A),

555 nuclear active SREBP1c (C) and SREBP2 (D), cytosolic inactive SREBP1c (F) and SREBP2 (G).

556 (B,E,H) Histograms report densitometric analysis of 6-8 mice per group. *$P<0.05$, **$P<0.01$,

557 ***$P<0.005$ vs CTRL; †$P<0.05$ vs FRT.

558

559 **Fig. 3. Expression analysis on markers of synthesis, β-oxidation and secretion of hepatic**

560 **lipids.** Western blotting analysis for ACC (A), HMGR (C), ApoB100 (E) and CPT1-L (G).

561 (B,D,F,H) Histograms report densitometric analysis of 6-8 mice per group. **$P<0.01$, ***$P<0.005$

562 vs CTRL; †$P<0.05$ vs FRT.

563

564 **Fig. 4. Expression analysis on RAGE/NFkB pathway**. Representative western blotting analysis

565 on total liver extracts for RAGE(A), on nuclear and cytosolic liver extracts showing NFkB

566 activation (C), on total liver extracts for ICAM-1 and CTGF (E). (B,D,F) Histograms report

567 densitometric analysis of 6-8 mice per group. *$P<0.05$, **$P<0.01$ vs CTRL.

568

569 **Fig. 5. Liver localization of SREBP1c, SCAP, CML, and MGO.** Representative 40x/100x

570 magnification photomicrographs of immunofluorescence analysis for SREBP1c (A,B), SCAP

571   (D,E), CML (G,I) and MGO (J,K) on 4μm cryostatic liver sections. To assess aspecific staining,

572   negative controls were prepared incubating sections only with secondary antibodies (anti-rabbit:

573   C,F; anti-mouse: I,L).

574

575   **Fig. 6. CML interaction with SCAP.** (A-F) Representative photomicrographs of double

576   immunofluorescence for SCAP/CML. SCAP (A,D) was revealed by red fluorescence and CML

577   (B,E) was revealed by green fluorescence. Colocalization is shown in merged images (C,E). (G)

578   Immunoprecipitation studies on liver extracts. SCAP has been immunoprecipitated (IP) and

579   membranes were incubated (IB) with anti-CML or anti-SCAP antibodies. (H) Histogram represent

580   CML to SCAP band density ratio obtained by densitometric analysis of immunoprecipitation

581   studies performed on 5-6 mice per group. Data are means ± S.D. Statistical significance: *$P<0.05$

582   vs CTRL; †$P<0.05$ vs FRT.

583

584

585

586

587

588

589

590

591

592

593

594

595

596

597 **Table 1. General parameters of mice after 30 weeks drinking water, FRT or GLC.** Data are

598 means ± S.D. of 8-10 mice per group. *$P<0.05$, **$P<0.01$, ***$P<0.005$ vs CTRL; †††$P<0.005$ vs
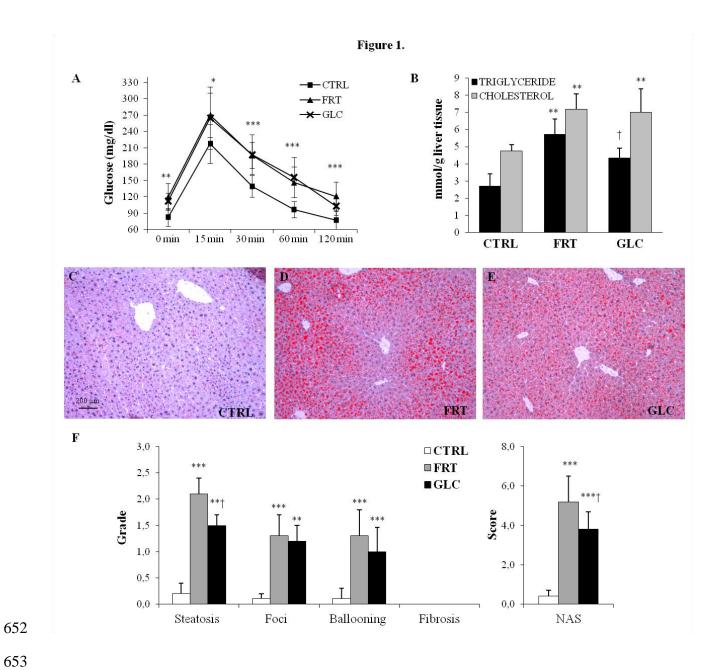
599 FRT.

	CTRL	FRT	GLC
Drink intake (ml/die)	3.7 ± 0.4	6.5 ± 0.5***	11.4 ± 3.8***†††
Food intake (g/die)	3.8 ± 0.9	2.6 ± 0.6*	2.0 ± 0.9**
Caloric intake (Kcal/die)	11.1 ± 2.8	11.3 ± 1.8	12.4 ± 2.1
Body weight increase (g)	12.4 ± 2.0	16.3 ± 2.5***	16.2 ± 2.4***
Fasting glycemia (mmol/l)	4.7 ± 1.0	7.2 ± 1.5**	7.1 ± 0.9***
Insulinemia (μg/l)	1.27 ± 0.07	2.13 ± 1.02	1.68 ± 1.03

600

601

602

603

604

605

606

607

608

609

610

611

612

613

614

615 **Table 2. Plasma lipid profile of mice after 30 weeks of water, FRT or GLC drinking.** Data are

616 means ± S.D. of 8-10 mice per group. *$P<0.05$, **$P<0.01$, ***$P<0.005$ vs CTRL; ††$P<0.01$ vs

617 FRT.

	CTRL	FRT	GLC
TG (mmol/l)	1.12 ± 0.18	1.60 ± 0.28**	1.34 ± 0.33
Cholesterol (mmol/l)	2.26 ± 0.20	3.10 ± 0.36***	2.68 ± 0.63
HDL (mmol/l)	1.46 ± 0.23	1.31 ± 0.24	1.23 ± 0.12*
LDL (mmol/l)	0.80 ± 0.17	1.44 ± 0.44**	0.95 ± 0.31
NEFA (mg/dl)	12.76 ± 1.58	9.75 ± 2.08**	15.29 ± 3.36*††

618

619
620

621

622

623

624

625

626

627

628

629

630

631

632

633

Table 3. Advanced glycated end-products evaluated by LC-MS in liver homogenates. Data are means ± S.D. of 8-10 mice per group. *$P<0.05$, **$P<0.01$, ***$P<0.005$ vs CTRL; †$P<0.05$, ††$P<0.01$, †††$P<0.005$ vs FRT.

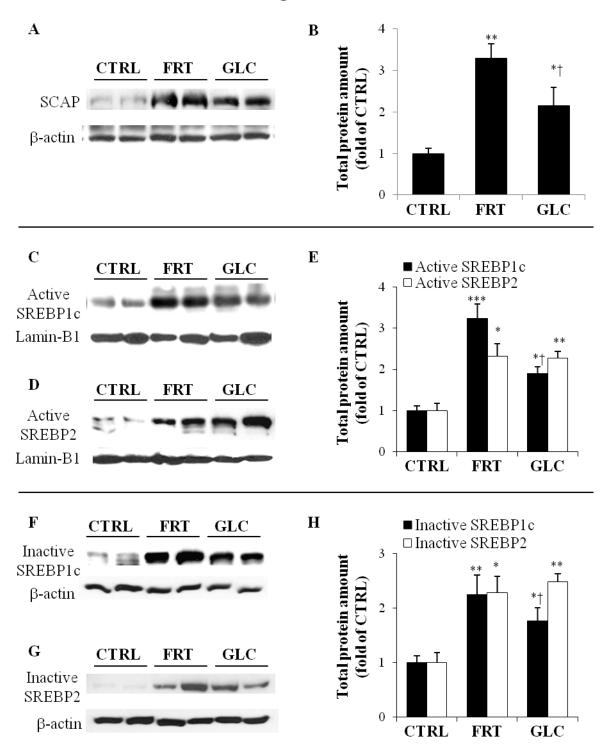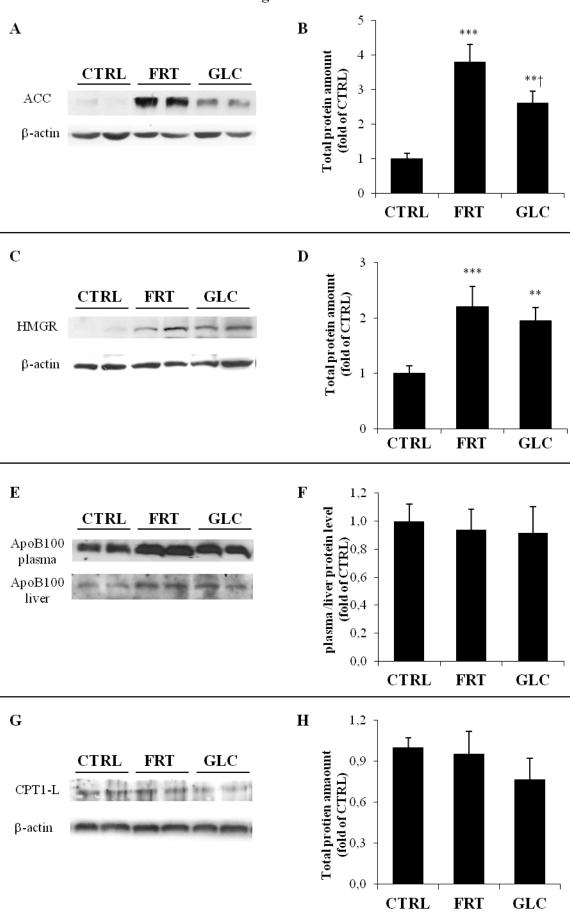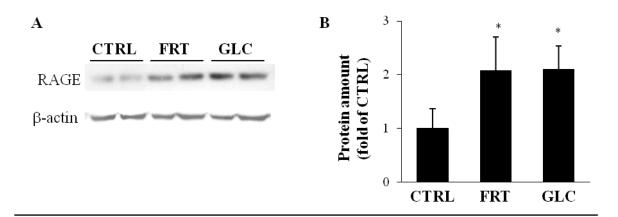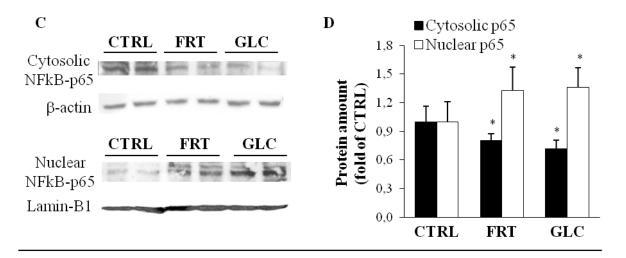|	CTRL	FRT	GLC
Pentosidine (pg/mg prot)	n.d.	$7.02 \pm 3.98^{*}$	$8.69 \pm 0.92^{***}$
GLAP (ng/mg prot)	n.d.	$0.36 \pm 0.09^{*}$	$2.20 \pm 0.86^{*\dagger}$
GOLD (ng/mg prot)	n.d.	$148.1 \pm 53.7^{**}$	$98.5 \pm 30.0^{**}$
MOLD (ng/mg prot)	n.d.	$0.37 \pm 0.24^{*}$	$1.08 \pm 0.11^{***\dagger\dagger}$
CML (ng/mg prot)	0.57 ± 0.09	$1.34 \pm 0.14^{***}$	$0.76 \pm 0.03^{*\dagger\dagger\dagger}$

Figure 1.

Figure 2.

Figure 3.

A

ACC

β-actin

CTRL   FRT   GLC

B

Total protein amount (fold of CTRL)

CTRL   FRT   GLC

*** (FRT) **† (GLC)

C

HMGR

β-actin

CTRL   FRT   GLC

D

Total protein amount (fold of CTRL)

CTRL   FRT   GLC

*** (FRT) ** (GLC)

E

ApoB100 plasma

ApoB100 liver

CTRL   FRT   GLC

F

plasma /liver protein level (fold of CTRL)

CTRL   FRT   GLC

G

CPT1-L

β-actin

CTRL   FRT   GLC

H

Total protien amaount (fold of CTRL)

CTRL   FRT   GLC

663

Figure 4.

A

CTRL   FRT   GLC

RAGE

β-actin

B

C

CTRL   FRT   GLC

Cytosolic
NFkB-p65

β-actin

CTRL   FRT   GLC

Nuclear
NFkB-p65

Lamin-B1

D

E

CTRL   FRT   GLC

ICAM-1

CTGF

β-actin

F

664

Figure 5.

SREBP1

SCAP

CML

MGO

665

Figure 6.